

GINZBURG-LANDAU SURFACE LIGHT BULLETS IN PHOTONIC LATTICES

D. MIHALACHE, D. MAZILU

*“Horia Hulubei” National Institute for Physics and Nuclear Engineering (IFIN-HH),
Department of Theoretical Physics,
407 Atomistilor, Magurele-Bucharest, 077125, Romania
E-mail: Dumitru.Mihalache@nipne.ro*

(Received March 9, 2009)

Abstract. We give an overview of recent results obtained in the study of discrete Ginzburg-Landau surface spatiotemporal optical solitons (“discrete Ginzburg-Landau surface light bullets”) in both one-dimensional and two-dimensional photonic lattices. We analyze spatiotemporal dissipative solitons near the edges of semi-infinite arrays of weakly coupled non-linear waveguides and in the corners or at the edges of truncated two-dimensional photonic lattices and demonstrate the existence of novel classes of continuous-discrete dissipative surface spatiotemporal optical solitons (“dissipative surface light bullets”). We study the existence and stability of these discrete Ginzburg-Landau surface light bullets and compare their properties with those of the spatiotemporal nonlinear modes located deep inside the one- and two-dimensional photonic lattices. We also describe the scenarios of the instability-induced dynamics of Ginzburg-Landau surface light bullets in both one-dimensional and two-dimensional photonic lattices.

Key words: spatiotemporal optical solitons, light bullets, discrete solitons, surface solitons, Ginzburg-Landau solitons, photonic lattices.

1. INTRODUCTION

In the past few decades there has been a huge amount of interest in the study of optical solitons, which defy either diffraction or dispersion and represent the particle-like counterpart of the more common nonlocalized (extended) light structures [1]-[6]. These localized structures of light are packets of electromagnetic radiation that propagate without spreading out despite diffraction or group-velocity dispersion (GVD). The supporting media that might sustain such localized self-guiding light structures should be nonlinear ones, that is, their refractive index should be dependent on the light intensity. Different types of optical nonlinearities, such as absorptive, dispersive, second-order (quadratic), third-order (cubic, Kerr-like), nonlocal, etc., can be used in practice to prevent either temporal dispersion or

spatial diffraction of light beams or both of them [7]-[86]. As a result, the field of either temporal or spatial optical solitons emerged from these fundamental studies of the interaction of intense laser beams with matter. The temporal/spatial optical solitons could be used as elementary bits of information in both sequential and parallel transmission and processing information systems.

However, there also exists a third kind of optical solitons, which are spatially confined pulses of light, the so-called spatiotemporal optical solitons [5], alias "light bullets" [7]. These spatiotemporal optical solitons are nondiffracting and nondispersing wavepackets propagating in nonlinear optical media. The three-dimensional (3D) spatiotemporal optical solitons are localized (selfguided) in the two transverse (spatial) dimensions and in the direction of propagation due to the balance of anomalous GVD of the medium in which they form and nonlinear self-phase modulation. Therefore, the "light bullet" is a fully 3D localized object in both space and time. The "light bullets" are the ideal candidates for the elementary bits of information in the future alloptical information processing systems due to their remarkable potential for massive parallelism (in space) and pipelining (in time) [5].

It should be mentioned that, while theoretical studies of both two-dimensional (2D) and 3D optical solitons have advanced a great deal in recent years, the reported experimental results remain more modest, being thus far limited to the experimental observation of 2D light bullets that overcome diffraction only in one transverse spatial dimension in quadratic nonlinear optical media [32].

In the 1980s a great deal of interest has been drawn to nonlinear optical surface waves guided by single and multiple interfaces separating different media. Quite often, features exhibited by such surface optical solitons have no analogue in the corresponding bulk media, which makes their study especially relevant. These electromagnetic waves are a purely nonlinear phenomenon with no counterpart in the linear limit; therefore they exist only if the mode power exceeds a certain threshold. Nonlinear transverse-electric, transversemagnetic, and mixed polarization surface waves traveling along single and multiple dielectric interfaces were theoretically predicted and systematically analyzed more than two decades ago [45]-[52]. However, direct observation of surface optical solitons has been hindered by huge experimental difficulties, related to their proper excitation and high power thresholds required for their formation.

Recently, the interest in the study of nonlinear self-trapped optical surface waves has been renewed after the theoretical predictions [53]-[55] and subsequent experimental demonstrations [56, 57] of nonlinearity-induced light localization near the edge of a truncated one-dimensional (1D) nonlinear waveguide array that can lead to the formation of the so-called discrete surface optical solitons. The generation of discrete surface solitons can be understood with the help of a simple physics [58] as a trapping of the optical field [4] near the repulsive edge of the lattice when the beam power exceeds some threshold value. These surface solitons

become possible solely due to discreteness effects and they exist in neither continuous nor linear limits. Some of the specific features of such discrete surface optical solitons in other relevant physical settings have been recently investigated both theoretically [59]-[61] and experimentally [62]-[65] (see also Ref. [66] for recent comprehensive overviews of experimental and theoretical developments in the area of discrete optical solitons).

The concept of surface optical solitons has been recently extended to the case of spatiotemporal surface solitons [67] described by the continuous-discrete nonlinear equations similar to those investigated earlier for cubic [68] and quadratic [69] nonlinear optical media, but with the properties strongly affected by the presence of the surface in the form of the lattice truncation.

Following our earlier studies [67], we recently considered both (2+1)-dimensional [39] and (3+1)-dimensional [40] continuous-discrete spatiotemporal models described by the complex Ginzburg-Landau (GL) equation. We thus investigated the effects of gain and loss due to optical amplifiers and saturable absorbers in truncated periodic photonic structures and we introduced *dissipative surface light bullets* [39, 40]. Similar to other types of discrete dissipative solitons in both one- and two-dimensional lattices [70]-[73], the dissipative surface light bullets exhibit novel features that, as a result of both discreteness and gain (loss) effects, have no counterpart in either continuous limit or in other conservative discrete models for both cubic and quadratic nonlinear media [74]-[79].

Moreover, localized modes on the surface of a three-dimensional dynamical lattice have been studied and the concept of surface solitons in three dimensions has been introduced [75]. Spatiotemporal vortices in optical fiber bundles were also investigated by means of the variational approximation and by using specific numerical methods [77]. Recently, the conditions for lowpower spatiotemporal quasisoliton formation in arrays of evanescently coupled silicon-on-insulator (SOI) photonic wires have been analyzed [76]. It was shown in Ref. [76] that pronounced soliton effects can be observed even in the presence of realistic loss, two-photon absorption, and higher-order GVD. The well established SOI technology offers an exciting opportunity in the area of spatiotemporal optical solitons because a strong anomalous GVD can be achieved with nanoscaled transverse dimensions and moreover, the enhanced nonlinear response resulting from this tight transverse spatial confinement of the electromagnetic field leads to soliton peak powers of only a few watts for 100-fs pulse widths (the corresponding energy being only a few hundreds fJ). The arrays of SOI photonic nanowires seem to be suitable for the observation of discrete surface light bullets because a suitable design of nanowires can provide dispersion lengths in the range of 1 mm and coupling lengths of a few millimeters (for 100-fs pulse durations) [76].

In this work we briefly overview some recent results obtained in the study of discrete Ginzburg-Landau surface spatiotemporal optical solitons (“discrete Ginzburg-Landau surface light bullets”) in both 1D and 2D photonic lattices. We

analyze spatiotemporal dissipative solitons near the edges of semi-infinite arrays of weakly coupled nonlinear waveguides and in the corners or at the edges of truncated two-dimensional photonic lattices. We study the existence, stability and robustness of these discrete Ginzburg-Landau surface light bullets and compare their properties with those of the spatiotemporal nonlinear modes located deep inside the one- and two-dimensional photonic lattices. We also describe different scenarios of instability-induced dynamics of Ginzburg-Landau surface light bullets in both 1D and 2D photonic lattices.

2. DISCRETE GINZBURG-LANDAU SURFACE LIGHT BULLETS IN TRUNCATED WAVEGUIDE ARRAYS

In this section we study the properties of the spatiotemporal Ginzburg-Landau solitons including the surface solitons located near the edge of a 1D array of optical waveguides in the presence of gain and loss. We find the domains of existence of such solitons in the relevant parameter space, for both on-site and inter-site spatiotemporal dissipative solitons and for the states localized at the different distances from the surface. We study the soliton stability and describe the complex instability-induced scenarios of the dynamics of discrete Ginzburg-Landau surface light bullets in truncated waveguide arrays.

In the following we consider a system of coupled GL equations that describes, in the framework of the tight-binding approximation of the coupled-mode theory, the spatiotemporal dynamics of a semi-infinite waveguide array in the presence of gain and loss,

$$\begin{aligned} -i \frac{\partial E_1}{\partial z} &= \tilde{D} \frac{\partial^2 E_1}{\partial t} + \alpha E_2 + F(E_1), \\ -i \frac{\partial E_n}{\partial z} &= \tilde{D} \frac{\partial^2 E_n}{\partial t^2} + \alpha (E_{n+1} + E_{n-1}) + F(E_n), \end{aligned} \quad (1)$$

where

$$F(E) = i\delta E + (p + q|E|^2)|E|^2 E, \quad (2)$$

and E_n is the amplitude of the electric field in the n -th waveguide ($n \geq 2$); the waveguide with $n=1$ designates the edge of the array and therefore $E_0 = 0$. In Eqs. (1) and (2) the real parameter $\delta > 0$ stands for linear losses and other coefficients of the discrete GL equation (1) are in general complex, and they are defined as follows: $\tilde{D} = D/2 - i\gamma$, $\alpha = \alpha_r + i\alpha_i$, $p = \sigma - i\varepsilon$, and $q = \nu + i\mu$. We scale the real part of \tilde{D} to 1/2, i.e. we consider anomalous group-velocity

dispersion (GVD) ($D = 1$) and scale the self-focusing Kerr nonlinearity coefficient to $\sigma = +1$. The imaginary part γ of the complex coefficient \tilde{D} accounts for the spectral filtering, i.e., dispersion of the linear loss. The real part α_r of the complex coefficient α is normalized to $1/2$; it accounts for tunneling between the adjacent waveguides, while the imaginary part α_i of the coefficient α stands for gain (losses) introduced by coupling. Here $\varepsilon > 0$ is the nonlinear (cubic) gain, $\mu > 0$ is the nonlinear (quintic) loss, while $\nu \leq 0$ accounts for the self-defocusing quintic correction to the cubic (Kerr) nonlinearity (saturation of the optical nonlinearity).

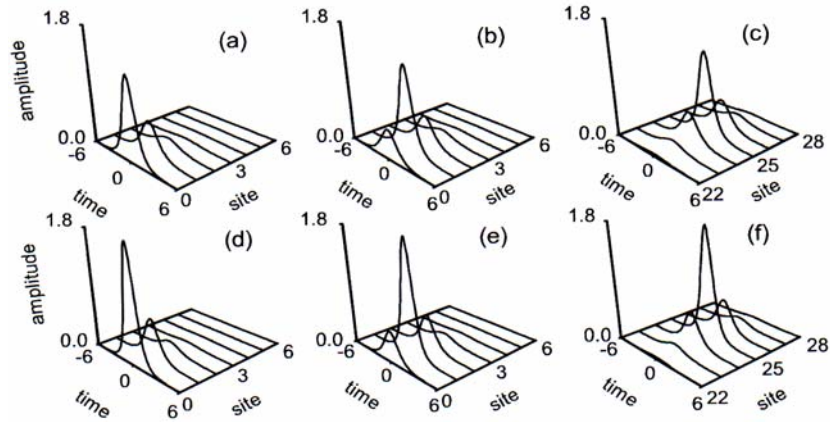


Fig. 1 – Examples of stable on-site discrete spatiotemporal surface solitons with both relatively low and relatively high peak amplitudes localized at distances of [(a) and (d)] $d = 0$, [(b) and (e)] $d = 1$, and [(c) and (f)] $d = 25$ from the edge of the waveguide array. Here $\delta = 1$, $\mu = 1$, and: a) $\varepsilon = 2.365$; b) $\varepsilon = 2.440$; c) $\varepsilon = 2.462$; d) $\varepsilon = 2.953$; e) $\varepsilon = 2.914$; f) $\varepsilon = 2.930$.

We look for spatiotemporal localized solutions of the discrete GL equations (1) and (2) in the form $E_n(t; z) = E_n(t) \exp(i\beta z)$, where β is the nonlinearity-induced shift of the waveguide propagation constant, and the envelope $E_n(t)$ describes the temporal evolution of the soliton-like pulse in the n -th waveguide. Although in a discrete model various combinations of the signs of dispersion and nonlinearity as well as the spatial topology may potentially lead to spatiotemporal localized solutions, here we restrict ourselves, for the sake of clarity and simplicity, to the case of anomalous GVD ($D = +1$), self-focusing nonlinearity ($\sigma = +1$) and the case of *in-phase* (*unstaggered*) solitons.

For this choice of parameters, we find numerically localized solutions $E_n(t)$ of the coupled GL equations (1) assuming that the amplitude of the pulses in each waveguide, $\max |E_n|$, decays rapidly far from the edge of the waveguide array, so that the corresponding solution describes a spatiotemporal mode localized near the surface.

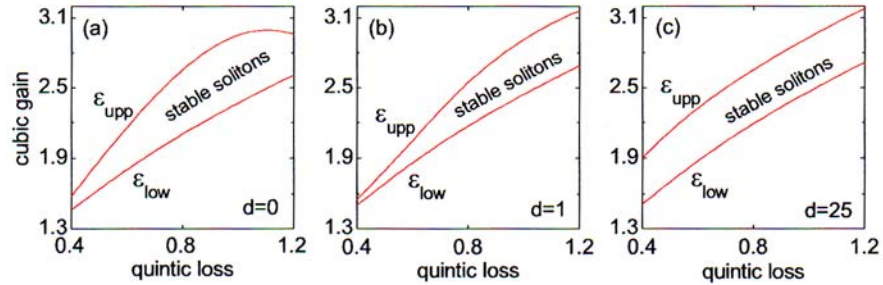


Fig. 2 – Domains of existence and stability in the plane (μ, ϵ) for on-site dissipative discrete surface light bullets located at distances of: a) $d = 0$; b) $d = 1$; c) $d = 25$ from the edge of the waveguide array. Here the linear loss coefficient $\delta = 1$.

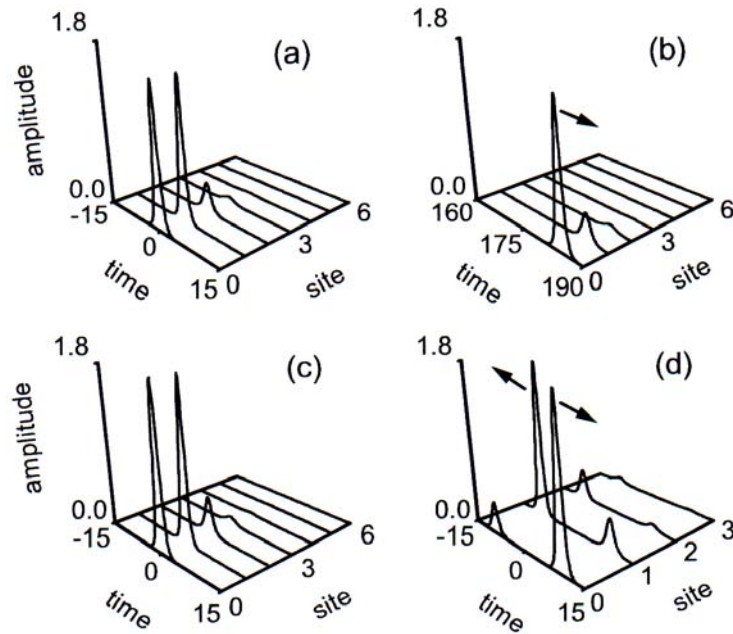


Fig. 3 – Reshaping of the relatively low-amplitude ((a) and (b)) unstable inter-site surface soliton centered at $d = 0$ into a moving low-power on-site soliton centered at the same site $d = 0$, and ((c) and (d)) splitting of the relatively high amplitude unstable inter-site soliton located at $d = 0$ into two, moving in opposite directions on-site solitons centered at $d = 0$ and $d = 1$. Here $\delta = 2$, $\mu = 1$, $\epsilon = 3.22$ ((a) and (b)), and $\epsilon = 3.5$ ((c) and (d)).

For simplicity, we fix some of the parameters of the GL model as follows: $\gamma = 0$, $\alpha_i = 0$, and $\nu = -0.1$, and vary the linear loss coefficient δ , the nonlinear gain ϵ , and the nonlinear (quintic) loss parameter μ . Thus we start with an arbitrary input pulse (typically, a Gaussian pulse), and simulate Eqs. (1) and (2) forward in z , expecting that a stable dissipative soliton localized at the edge of the waveguide array would

emerge after a certain propagation distance in the form of $E_n(t; z) = E_n(t) \exp(i\beta z)$, where the propagation constant β is the corresponding eigenvalue determined by the parameters of Eqs. (1) and (2). We employ a standard Crank-Nicolson scheme for numerical integration, with typical transverse and longitudinal step-sizes $\Delta t = 0.1$ and $\Delta z = 0.01$. The nonlinear finite-difference equations are solved by using the Picard iteration method and the resulting linear system is handled with the help of the Gauss-Seidel iterative procedure. To achieve good convergence, we typically need ten Picard and four Gauss-Seidel iterations. The propagation constant β is determined as the z -derivative of the phase of $E_n(t, z)$, and the solution is reckoned to achieve a stationary form if β ceases to depend on z and t , up to five significant digits.

Next we show in Fig. 1 several examples of relatively low peak amplitude (top panels in Fig. 1) and relatively high peak amplitude (bottom panels in Fig. 1) stable *odd* (on-site) nonlinear spatiotemporal continuous-discrete dissipative localized states, that can be termed 'discrete dissipative surface light bullets' (discrete Ginzburg-Landau surface light bullets). In Fig. 1 we have fixed the values of the parameters δ (linear loss) and μ (nonlinear quintic loss) and we have varied the parameter ε (nonlinear cubic gain). The low peak amplitude solitons corresponds to relatively small values of the nonlinear cubic gain parameter ε (near to the lower limit of their existence domain), whereas the high peak amplitude solitons corresponds to relatively large values of the nonlinear cubic gain parameter ε (near to the upper limit of their existence domain), see Fig. 2 below. We mention that similar shapes of the on-site solitons can be obtained for other parameter sets, too. These localized solutions are centered at the edge waveguide ($d = 0$), or near to the edge waveguide ($d = 1$), etc., and they describe the discrete Ginzburg-Landau surface light bullets [39]. As a matter of fact, these localized modes are a generalization to dissipative dynamical systems of the spatiotemporal surface solitons recently predicted to exist in non-dissipative (Hamiltonian) semi-infinite discrete dynamical systems [67]. Importantly, for larger values of d the properties of such discrete GL light bullets do not depend on the surface, so they converge to the continuous-discrete spatiotemporal GL solitons in infinite chains [39].

The discrete GL spatiotemporal optical solitons can be characterized by the total power defined as

$$P = \sum_{n=1}^{\infty} \int_{-\infty}^{+\infty} |E(t)|^2 dt, \quad (3)$$

which remains constant for stationary solitons [39].

The on-site spatiotemporal dissipative surface solitons exist and are stable in some intervals of the variation of the cubic gain ε . In fact, there exists a minimum value ε_{low} of the nonlinear gain ε for supporting a stable soliton; for the values of ε

smaller than the minimum value ε_{low} the input pulse decay to nil. For values of the cubic gain parameter inside the stability interval $[\varepsilon_{\text{low}}, \varepsilon_{\text{upp}}]$ a Gaussian input rapidly converges to the corresponding on-site discrete surface soliton and its propagation constant β can be uniquely determined. However, for values of the nonlinear gain parameter ε larger than a maximum value ε_{upp} , the dissipative soliton cannot be formed as well; in this case the soliton propagation constant β cannot be determined numerically. Actually for the values of the cubic gain ε beyond the upper limit ε_{upp} the peak amplitude and the power increases indefinitely in an oscillatory manner [39]. In this case we get the conversion of the Gaussian input into an expanding pattern composed of two fronts moving in opposite directions along the temporal axis, similar to the case of dissipative spatiotemporal solitons in the continuous limit [37, 38].

In Fig. 2 we show typical domains of existence and stability of on-site dissipative solitons in the plane (μ, ε) for $\delta = 1$. We have also investigated the influence of the variation of the parameter δ on these domains; we have found that by increasing the parameter δ , the existence and stability bands in Fig. 2 translates to higher values of the cubic gain parameter ε . However, if we keep fixed the parameter δ and decrease the quintic loss parameter μ , the existence domains of both in-site and intra-site solitons shifts to lower values of the cubic gain parameter ε , accompanied by an increase in the power threshold for the soliton existence. For example, for $\delta = 2$, the on-site soliton centered at $d = 0$ has a power threshold $P_{th} \approx 4.14$ and an existence and stability interval $1.986 < \varepsilon < 2.368$ for $\mu = 0.4$, as compared to the values $P_{th} \approx 2.855$, and $3.155 < \varepsilon < 3.767$ for $\mu = 1$.

The stability of the odd and even spatiotemporal surface GL solitons has been investigated by performing the linear stability analysis (via the calculation of the perturbation eigenvalues) and by checking in direct simulations the outcome of the linear stability analysis. To this aim we have considered a perturbed solution of the form [39]:

$$E_n(t, z) = [E_n(t) + f_n(t) \exp(\lambda z)] \exp(i\beta z), \quad (4)$$

where λ (that may be, in general, a complex number) is the growth rate of the small perturbation represented by the eigenmode f_n .

The substitution of the above expression into the coupled system of GL equations (1) leads to linearized equations for the perturbation eigenmodes f_n and perturbation eigenvalues λ , which were solved by standard numerical techniques. We have found that for the on-site solitons $\max \text{Re}(\lambda) = 0$, implying their stability in the whole domain of their existence, whereas the inter-site solitons were found to be unstable in the whole domain of their existence, because $\max \text{Re}(\lambda) > 0$ [39].

Moreover, we have cross-checked the outcome of the linear stability analysis by employing direct simulations of the propagation dynamics. We have found that the on-site dissipative solitons survive in the presence of relatively large (20%) white input noise added on the stationary solutions, whereas the inter-site solitons are indeed unstable. We have analyzed systematically the possible outcomes of the evolution of the unstable inter-site surface solitons centered at distance $d = 0$ from the edge of the waveguide array, which were propagated in the lack of input noise. As a typical example we have fixed the parameters $\delta = 2$ and $\mu = 1$, and we have varied the cubic gain parameter ε . Recall that for this set of parameters the inter-site solitons exist in the interval $\varepsilon_{low} = 3.130 < \varepsilon < 3.637 = \varepsilon_{upp}$. We have found that for relatively low values of the cubic gain parameter in the vicinity of the minimum permitted value ε_{low} the input unstable inter-site solitons decay to nil. If we increase the cubic gain, e. g., to the value $\varepsilon = 3.22$, the relatively low peak-amplitude unstable inter-site soliton centered at $d = 0$ eventually reshape to a moving low power stable on-site surface soliton (again centered at $d = 0$), which corresponds to the same set of parameters of the GL equation (Figs. 3(a) and 3(b)). However, for larger values of the cubic gain, the relatively high peak-amplitude unstable inter-site soliton centered at $d = 0$ splits into two *moving in opposite directions*, stable on-site solitons, centered at two consecutive sites ($d = 0$ and $d = 1$), corresponding to the same set of parameters of the GL equation (Figs. 3(c) and 3(d)). Finally, for relatively large values of the cubic gain parameter in the vicinity of the maximum permitted value ε_{upp} the input unstable inter-site soliton generates an expanding pattern composed of two fronts moving in opposite directions along the temporal axis (the corresponding power increases indefinitely) [39].

3. DISCRETE GINZBURG-LANDAU SURFACE LIGHT BULLETS IN TWO-DIMENSIONAL PHOTONIC LATTICES

In this section, we study the properties of discrete Ginzburg-Landau surface light bullets including surface spatiotemporal solitons located in the corners or at the edges of the truncated two-dimensional photonic lattice in the presence of gain and loss. We find the domains of existence of such dissipative surface light bullets in the relevant parameter space, for both on-site and inter-site spatiotemporal dissipative solitons located in the corner, edge and the center of the lattice. We study the stability of spatiotemporal Ginzburg-Landau solitons and describe the complex instability-induced scenarios of their dynamics in two-dimensional photonic lattices [40].

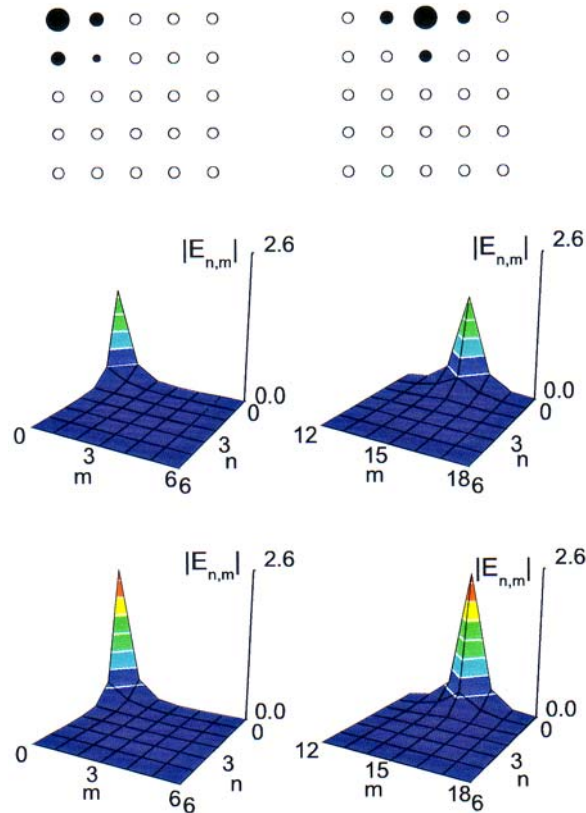


Fig. 4 – Examples of spatial cross sections of stable on-site spatiotemporal surface solitons with both relatively low and relatively high peak amplitudes localized in the lattice corner (left column) and at the lattice edge (right column). Parameters are: $\mu = 1$ and $\varepsilon = 3.5$ (for low amplitude solitons); $\mu = 0.2$ and $\varepsilon = 1.5$ (for high amplitude solitons).

We consider light propagation in a square photonic lattice created by weakly coupled arrays of identical evenly spaced two-dimensional homogeneous waveguides, which we model in the framework of the coupled-mode approach. In the discrete model the electric field is decomposed into modes of identical waveguides with the mode profile $\mathbf{e}(x, y, \omega_0)$, and the normalized (with respect to the coupling constant) propagation constant k_z at the center frequency of the pulse ω_0 as

$$\mathbf{E}(x, y, z, t) = \sum E_{n,m}(t, z) \mathbf{e}(x, y, \omega_0) \exp[i(k_z z - \omega_0 t)] + c.c., \quad (5)$$

where the propagation distance z is normalized with respect to the coupling constant in both horizontal and vertical directions, and t is the time normalized with respect to the ratio of group velocity dispersion and coupling constant.

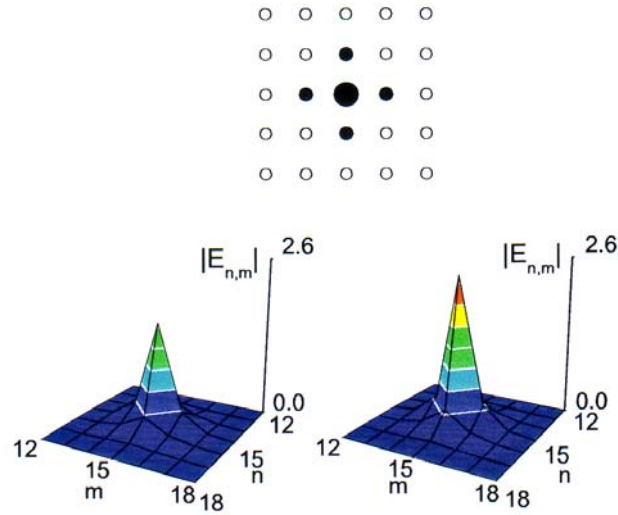


Fig. 5 – Spatial cross sections of stable on-site spatiotemporal solitons with low and high peak amplitudes localized in the center of the lattice. Parameters are: $\mu = 1$ and $\varepsilon = 3.5$ (left), $\mu = 0.2$ and $\varepsilon = 1.5$ (right).

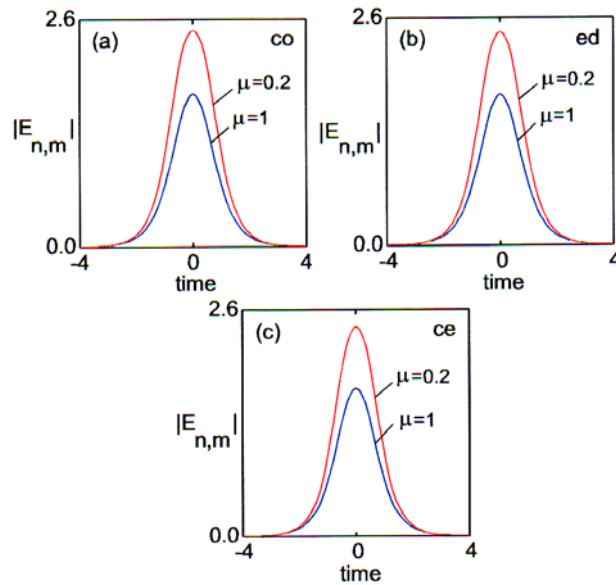


Fig. 6 – Temporal cross-sections of stable on-site spatiotemporal surface solitons localized in the corner, at the edge, and in the center of the lattice, respectively. Shown are the temporal profiles of relatively low-amplitude and relatively high-amplitude solitons corresponding to the spatial profiles displayed in Figs. 4 and 5. Here $\varepsilon = 3.5$ (for low amplitude solitons) and $\varepsilon = 1.5$ (for high amplitude solitons).

In the coupled-mode theory, only the amplitude $E_{n,m}$ of the electric field in the waveguide with the site (n, m) is considered to evolve during propagation while the mode profile is assumed to remain constant. Therefore, the slowly varying normalized envelope $E_{n,m}$ obeys a set of coupled partial differential equations which describes, in the framework of the tight-binding approximation (or coupled mode theory), the spatiotemporal dynamics of light in a two-dimensional waveguide lattice in the presence of gain and loss [40],

$$i \frac{\partial E_{n,m}}{\partial z} + \tilde{D} \frac{\partial^2 E_{n,m}}{\partial t^2} + \alpha (V_n + V_m) E_{n,m} + F(E_{n,m}) = 0, \quad (6)$$

where

$$F(E) = i\delta E + (p + q|E|^2)|E|^2 E, \quad (7)$$

Here the lattice indices are $n, m = 0, 1, \dots$, $E_{-1,m} = E_{n,-1} \equiv 0$ due to the lattice termination. We define the lattice couplings as: $V_n E_{n,m} = E_{1,m}$, for $n = 0, m \geq 0$ and $V_n E_{n,m} = E_{n+1,m} + E_{n-1,m}$, for $n > 0$, respectively, $V_m E_{n,m} = E_{n,1}$ for $m = 0, n \geq 0$ and $V_m E_{n,m} = E_{n,m+1} + E_{n,m-1}$, for $m > 0$.

The real parameter $\delta > 0$ stands for linear losses. Other coefficients of the discrete Ginzburg-Landau equation (6) are assumed, in general, to be complex, and they are defined as follows: $\tilde{D} = D/2 - i\gamma$, $\alpha = \alpha_r + i\alpha_i$, $p = \sigma - i\varepsilon$, and $q = \nu + i\mu$. We scale the real part of \tilde{D} to 1/2, i.e. we consider anomalous GVD ($D = +1$), and scale the self-focusing Kerr nonlinearity coefficient to $\sigma = +1$. The imaginary part γ of the complex coefficient \tilde{D} accounts for the spectral filtering, i.e. dispersion of the linear loss. The real part α_r of the complex coefficient α is normalized to 1/2; it accounts for tunneling between the adjacent waveguides, while the imaginary part α_i of the coefficient α stands for gain (losses) introduced by coupling. Here $\varepsilon > 0$ is the nonlinear (cubic) gain, $\mu > 0$ is the nonlinear (quintic) loss, while $\nu \leq 0$ accounts for the self-defocusing quintic correction to the cubic (Kerr) nonlinearity (saturation of the optical nonlinearity), see Ref. [40].

Here we are restricting to the case of anomalous GVD ($D = +1$) and self-focusing cubic nonlinearities ($\sigma = +1$), because we are considering only the existence and stability of *bright-type* discrete spatiotemporal Ginzburg-Landau solitons. However, such bright-type discrete spatiotemporal solitons should also exist in the case of normal GVD ($D = -1$) and for self-defocusing cubic nonlinearities ($\sigma = -1$) [67]. In order to get stable bright-type solitons, a stable supporting zero background is necessary; therefore we have considered that the parameter δ accounting for linear losses is positive [40].

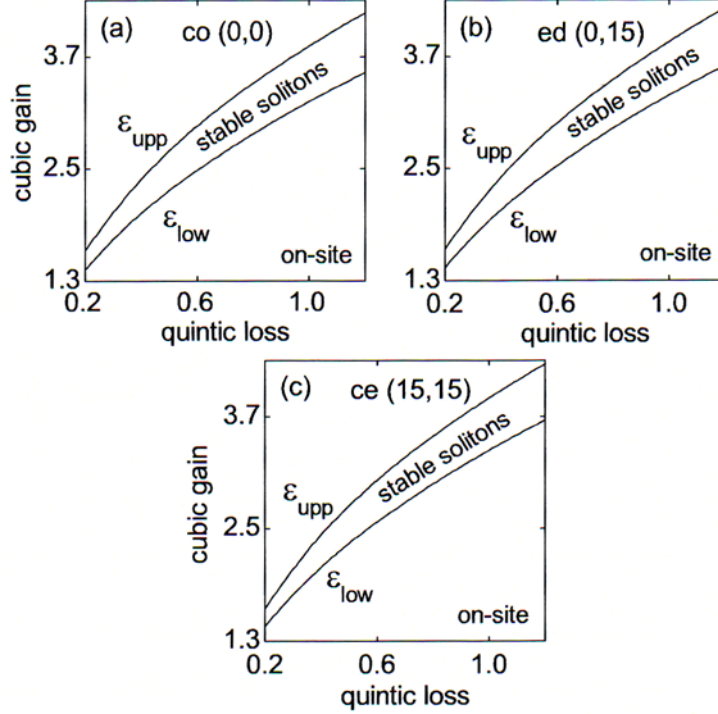


Fig. 7 – Domains of existence and stability in the plane (μ, ε) for on-site dissipative discrete light bullets located in the corner (co), at the edge (ed), and in the center (ce), respectively.

Next we look for spatiotemporal localized solutions of the discrete GL equations (6) and (7) in the form

$$E_{n,m}(t, z) = E_{n,m}(t) \exp(i\beta z), \quad (8)$$

where β is the nonlinearity-induced shift of the waveguide propagation constant, and the envelope $E_{n,m}(t)$ describes the temporal evolution of the solitonlike pulse propagating in the (n, m) waveguide lattice site. Although in a discrete model various combinations of the signs of dispersion and nonlinearity as well as the spatial topology may potentially lead to different types of spatiotemporal localized solutions, in this paper we restrict ourselves, for the sake of clarity and simplicity, to the case of anomalous GVD ($D = +1$), self-focusing nonlinearity ($\sigma = +1$), and in-phase (unstaggered) localized modes in two-dimensional dissipative lattices.

The localized solutions $E_{n,m}(t)$ of the partial differential equations (6) are found by adequate numerical methods assuming that the amplitude of the pulses in each waveguide, $\max |E_{n,m}|$, decays rapidly far from the corners and the edges of the truncated waveguide lattice, so that the corresponding solution describes a

spatiotemporal mode localized in the lattice corner or at its edge (for more details about the numerical techniques used to get stationary localized solutions, see Ref. [40]). Also we find numerically the nonlinear discrete spatiotemporal GL solitons located far away from the corners and edges, so such modes can be therefore treated as the modes of an infinite two-dimensional photonic lattice.

For the numerical calculations we fixed, for simplicity, some of the parameters of the GL model as follows: $\gamma = 0$, $\alpha_i = 0$, $\nu = -0.1$, $\delta = 2$ and varied the nonlinear (cubic) gain ε , and the nonlinear (quintic) loss μ [40]. In order to find numerically the envelope $E_{n,m}(t)$ of the spatiotemporal dissipative soliton we started with an arbitrary input pulse (typically, a Gaussian one), and simulated Eqs. (6) and (7) forward in z , expecting that a stable dissipative soliton localized at the corner, edge or deep inside the photonic lattice would emerge after a certain propagation distance in the form of $E_{n,m}(t, z) = E_{n,m}(t) \exp(i\beta z)$, where the propagation constant β is the corresponding eigenvalue determined by the parameters of Eqs. (6) and (7). As in the case of spatiotemporal surface GL solitons in 1D photonic lattices [39], we employed a standard Crank-Nicolson scheme for numerical integration of the coupled complex GL equations; the temporal grid had a typical step length $\Delta t = 0.1$, whereas the typical longitudinal step size was $\Delta z = 0.01$. Depending on the value of the propagation constant, we used up to 161 discretization points in the continuous time interval $[0, t_{\max}]$, and up to 31×31 grid points for the discrete spatial coordinates. The nonlinear finite-difference equations were solved by using the Picard iteration method, and the resulting linear system was handled with the help of the Gauss-Seidel iterative procedure [40]. To achieve good convergence, we typically needed ten Picard and four Gauss-Seidel iterations. The propagation constant β was determined as the z -derivative of the phase of $E_{n,m}(t, z)$, and the solution was reckoned to achieve a stationary form if β ceases to depend on z and t , up to five significant digits (see Ref. [40]).

Typical examples of spatial profiles and temporal cross-sections of stable *on-site* (odd) spatiotemporal GL solitons located in the corners or at the edges of the two-dimensional photonic lattice together with the solitons localized in the center of the lattice (representing a spatiotemporal discrete soliton in an infinite two-dimensional photonic lattice), are shown in Figs. (4)-(6) for two representative sets of the parameters (μ, ε) . These nonlinear spatiotemporal continuous-discrete dissipative localized states can be termed 'discrete dissipative surface light bullets' (discrete Ginzburg-Landau surface light bullets) [40]. We mention that similar shapes of the on-site solitons are obtained for other parameter sets, too. The rule of thumb is the following one: when the nonlinear quintic loss μ is fixed the amplitude (and energy) of the soliton increases as the nonlinear cubic gain ε grows, whereas when the cubic gain parameter is fixed the amplitude (and energy) of the soliton increases as the quintic loss parameter decreases.

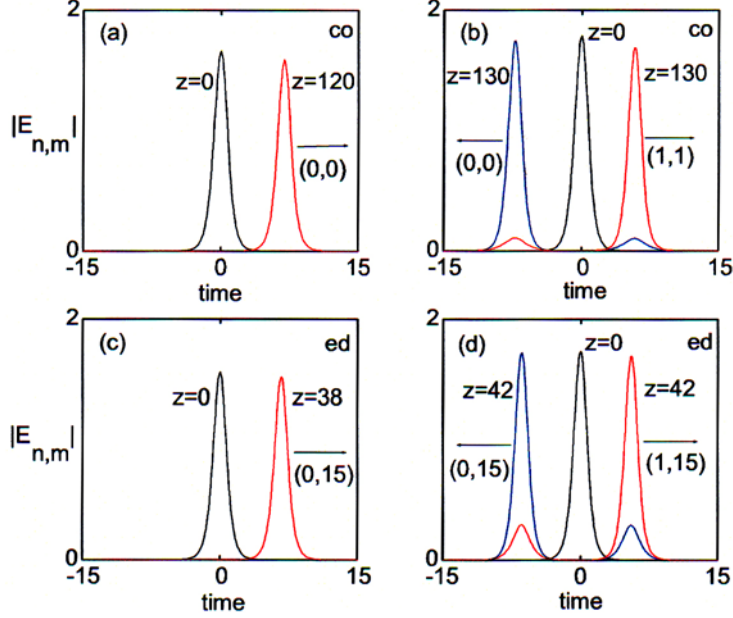


Fig. 8 – Reshaping of the relatively low-amplitude unstable inter-site (a) (0, 0) corner and (c) (0, 15) edge solitons into moving low-energy on-site corner and edge solitons, respectively, centered at the same lattice sites, and splitting of the relatively high amplitude unstable inter-site (b) corner and (d) edge solitons into two moving in opposite directions on-site solitons localized at different lattice sites. Here $\mu = 1$, $\varepsilon = 3.3$ (a,c), and $\varepsilon = 3.5$ (b,d).

As in the case of 1D photonic lattices, the dissipative optical solitons can be characterized by the total energy \mathcal{E} defined as

$$\mathcal{E} = \sum_{n,m} \int_{-\infty}^{+\infty} |E_{n,m}(t)|^2 dt \quad (9)$$

which remains constant for stationary dissipative solitons. If we compare the corresponding energy curves of different surface modes including the case of a spatiotemporal soliton located inside the lattice, we notice that in a large domain of variation of the nonlinear (cubic) gain ε , the energy of surface modes localized in the corners and at the edges of the lattice is lower than that of the bulk mode [40], similar to the case of surface light bullets in the corresponding conservative system [67].

As concerning the stability of these discrete surface Ginzburg-Landau light bullets, we found that the on-site spatiotemporal dissipative solitons located in the corner (co), at the edge (ed), and in the center (ce) of the lattice are stable in some intervals of the variation of the cubic gain ε (Fig. 7). In fact, we find that there exists a minimum value ε_{low} of the nonlinear gain ε for supporting a stable soliton. Indeed, for the values of ε smaller than the minimum value ε_{low} the input pulse

decays whereas for the values of the cubic gain parameter inside the stability interval $[\varepsilon_{\text{low}}, \varepsilon_{\text{upp}}]$ a Gaussian input rapidly converges towards the corresponding on-site discrete surface soliton, and its propagation constant β can be uniquely determined. However, for values of the nonlinear gain parameter ε larger than a maximum value ε_{upp} , a dissipative soliton cannot be formed as well; in this case the soliton propagation constant β cannot be determined numerically [the peak amplitude and the energy increases indefinitely in an oscillatory manner]. A Gaussian input is converted into an expanding pattern composed of two fronts moving in the opposite directions along the temporal axis, similar to the case of dissipative spatiotemporal surface solitons in 1D waveguide arrays [39]. We mention that stability domains similar to those shown in Figs. 7(a,b) for the (0, 0) corner and (0, 15) edge solitons can be found for the (1, 1) corner and (1, 15) edge solitons as well.

The stability of the on-site (odd) and inter-site (even) spatiotemporal surface GL solitons has been investigated by performing a linear stability analysis (via the calculation of the perturbation eigenvalues) and by double-checking these results in direct propagation simulations. To this aim we have considered a perturbed solution of the nonlinear dynamical system (6) of the form:

$$E_{n,m}(t; z) = [E_{n,m}(t) + f_{n,m}(t) \exp(\lambda z)] \exp(i\beta z), \quad (10)$$

where λ (that may be, in general, a complex number) is the growth rate of the small perturbation represented by the eigenmode $f_{n,m}$.

The substitution of the above expression into the coupled system of GL equations (6) leads to linearized equations for the perturbation eigenmodes $f_{n,m}$ and perturbations eigenvalues λ , which were solved by standard numerical techniques. We have found that for the on-site solitons $\max \text{Re}(\lambda) = 0$, implying their stability in the whole domain of their existence, whereas doublepeak corner and edge inter-site solitons were found to be unstable in the whole domain of their existence, because $\max \text{Re}(\lambda) > 0$. However, the stability of multiple-peaked inter-site GL solitons located deep in the center of the twodimensional lattice deserves a separate study.

Though the on-site center solitons were found to be stable in the whole domain of their existence, the two-peaked inter-site center solitons were found to be either stable or unstable, depending on the values of the two relevant parameters of the GL model, namely μ and ε . We expect to get also domains of stability for four-peaked inter-site spatiotemporal GL solitons located deep inside the lattice, similar to the case of spatial discrete GL solitons in twodimensional photonic lattices [73].

Notice that in addition to the fundamental on-site (0; 0) corner soliton, other on-site corner solitons centered in the (1; 1) and (2, 2) lattice sites are found to be stable in their whole existence domain. Moreover, we have found that in addition to the fundamental on-site (0, 15) edge soliton, other onsite edge solitons centered

in the (1, 15) and (2, 15) lattice sites are found to be stable in their whole existence domain. Moreover, we have found that the out-of-phase (staggered) discrete spatiotemporal Ginzburg-Landau solitons are unstable [40].

In order to cross-check the results of our linear stability analysis, we employed direct numerical simulations to study the propagation dynamics of both stable and unstable solitons. We found that the on-site dissipative solitons survived in the presence of a relatively large (up to 10%) white input noise added to the stationary solutions, whereas the inter-site solitons, for which the linear stability analysis predicts the existence of a nonzero real part of the perturbation eigenvalue, were found to be indeed unstable in numerical propagation simulated without adding a white noise at the input.

As the next step, we analyzed systematically the possible outcomes of the evolution of the unstable double-peak inter-site solitons localized at the corner or at the edge or the center, which are propagated without an input noise. We fixed the parameter $\mu = 1$ and varied the cubic gain parameter ε . Recall that for our choice of parameters the inter-site corner and edge solitons exist in the intervals $\varepsilon_{low} = 3.185 < \varepsilon < 3.743 = \varepsilon_{upp}$, and $\varepsilon_{low} = 3.262 < \varepsilon < 3.746 = \varepsilon_{upp}$, respectively. We found that, for relatively low values on the cubic gain parameter in the vicinity of the minimum permitted value ε_{low} , the input unstable inter-site corner and edge solitons decay. If we increase the cubic gain, e.g., to the value $\varepsilon = 3.3$, the relatively low peakamplitude unstable inter-site solitons localized in the corner and at the edge eventually reshape to *moving* low-energy stable on-site (0, 0) corner and (0, 15) edge solitons, which correspond to the same set of parameters of the GL equation (Figs. 8(a) and 8(c)). However, for larger values of the cubic gain (e.g., for $\varepsilon = 3.5$) the relatively high peak-amplitude unstable inter-site corner and edge solitons split into two *moving into the opposite directions* stable on-site corner and edge solitons, centered in two different lattice sites (0, 0) and (1, 1), respectively (0, 15) and (1, 15). These emerging pairs of stable on-site solitons (Figs. 8(b) and 8(d)) correspond to the same set of parameters of the GL equation. Finally, for relatively large values of the cubic gain parameter in the vicinity of the maximum permitted value ε_{upp} , the input unstable inter-site solitons generate expanding patterns composed of two fronts moving in opposite directions along the temporal axis (the corresponding energy increases indefinitely). As concerning the instability scenarios of the two-peak inter-site solitons located deep inside the lattice (the bulk mode) we have found that the unstable inter-site (15, 15) center soliton decay into a stable on-site (0, 15) edge soliton [40].

4. CONCLUSIONS

In this work we overviewed some recent results concerning the existence, stability and robustness of discrete Ginzburg-Landau surface spatiotemporal optical solitons (“discrete Ginzburg-Landau surface light bullets”). We analyzed

spatiotemporal light localization near the edges of semi-infinite arrays of weakly coupled nonlinear waveguides and in the corners or at the edges of truncated two-dimensional photonic lattices and demonstrated the existence of novel classes of continuous-discrete Ginzburg-Landau surface spatiotemporal optical solitons (continuous-discrete dissipative surface light bullets). We studied these discrete Ginzburg-Landau surface light bullets and compared their unique features with those of the Ginzburg-Landau spatiotemporal nonlinear modes located deep inside the photonic lattices.

Another issue of much interest is the study of collisions between discrete surface spatiotemporal solitons in both nonlinear waveguide arrays and in two-dimensional photonic lattices. Recently we analyzed the outcomes of collisions between continuous-discrete spatiotemporal surface solitons in truncated waveguide arrays [87]. Since these solitons can be located at different distances from the edge of the waveguide array, we observed a variety of collision scenarios and different outcomes. Thus in addition to well-known scenarios of soliton fusion and symmetric scattering, we got strongly asymmetric outcomes [87]. These preliminary studies can be easily extended to the case of collisions between discrete surface spatiotemporal solitons in two-dimensional photonic lattices. Another open problem is the study of collisions between discrete Ginzburg-Landau surface light bullets in both one-dimensional and two-dimensional photonic lattices.

Acknowledgements. Part of the research work overviewed in this paper has been carried out in collaboration with Falk Lederer and Yuri S. Kivshar. We are deeply indebted to them.

REFERENCES

1. N. Akhmediev, A. Ankiewicz (Eds.), *Dissipative Solitons: From Optics to Biology and Medicine*, Lect. Notes Phys., **751**, Springer, Berlin, 2008.
N. Akhmediev, A. Ankiewicz (Eds.), *Dissipative Solitons*, Lect. Notes Phys., **661**, Springer, Berlin, 2005.
2. N. N. Akhmediev, A. Ankiewicz, *Solitons: Nonlinear Pulses and Beams*, London, Chapman and Hall, 1997.
3. G. I. Stegeman, D. N. Christodoulides, M. Segev, *IEEE J. Select. Top. Quant. Electron.*, **6**, 1419 (2000).
4. Y. S. Kivshar, G. P. Agrawal, *Optical solitons: From fibers to photonic crystals*, Academic Press, San Diego, 2003.
5. B. A. Malomed, D. Mihalache, F. Wise, L. Torner, *J. Opt. B: Quantum Semiclassical Opt.*, **7**, R53 (2005).
6. D. Mihalache, D. Mazilu, *Rom. Rep. Phys.*, **60**, 957 (2008).
7. Y. Silberberg, *Opt. Lett.*, **15**, 1282 (1990).
8. L. Bergé, *Phys. Rep.*, **303**, 260 (1998);
V. V. Konotop, P. Pacciani, *Phys. Rev. Lett.*, **94**, 240405 (2005).

9. I. Towers, B. A. Malomed, *J. Opt. Soc. Am. B*, **19**, 537 (2002).
10. D. Edmundson, R. H. Enns, *Opt. Lett.*, **17**, 586 (1992);
N. Akhmediev, J. M. Soto-Crespo, *Phys. Rev. A*, **47**, 1358 (1993);
R. McLeod, K. Wagner, S. Blair, *Phys. Rev. A*, **52**, 3254 (1995).
11. B. A. Malomed *et al.*, *Phys. Rev. E*, **56**, 4725 (1997).
12. D. V. Skryabin, W.J. Firth, *Opt. Commun.*, **148**, 79 (1998).
13. L. Torner, D. Mazilu, D. Mihalache, *Phys. Rev. Lett.*, **77**, 2455 (1996);
D. Mihalache, F. Lederer, D. Mazilu, L.-C. Crasovan, *Opt. Eng.*, **35**, 1616 (1996);
D. Mihalache, D. Mazilu, L.-C. Crasovan, L. Torner, *Opt. Commun.*, **137**, 113 (1997);
D. Mihalache *et al.*, *Phys. Rev. E*, **62**, R1505 (2000).
14. D. Mihalache *et al.*, *Opt. Commun.*, **152**, 365 (1998);
Opt. Commun., **169**, 341 (1999); *Opt. Commun.*, **159**, 129 (1999); *Phys. Rev. E*, **62**, 7340 (2000);
N.-C. Panoiu *et al.*, *Phys. Rev. E*, **71**, 036615 (2005).
15. D. Mihalache *et al.*, *Phys. Rev. Lett.*, **88**, 073902 (2002);
D. Mihalache *et al.*, *Phys. Rev. E*, **66**, 016613 (2002);
H. Michinel, M. J. Paz-Alonso, V. M. Perez-Garcia, *Phys. Rev. Lett.*, **96**, 023903 (2006);
D. Mihalache, D. Mazilu, L.-C. Crasovan, B. A. Malomed, F. Lederer *Phys. Rev. E*, **61**, 7142 (2000);
A. Desyatnikov, A. Maimistov, B. Malomed, *Phys. Rev. E*, **61**, 3107 (2000).
16. L. Torner *et al.*, *Opt. Commun.*, **199**, 277 (2001).
17. I. V. Mel'nikov, D. Mihalache, N.-C. Panoiu, *Opt. Commun.*, **181**, 345 (2000).
18. M. Blaauboer, B. A. Malomed, G. Kurizki, *Phys. Rev. Lett.*, **84**, 1906 (2000).
19. W. Krolikowski, O. Bang, *Phys. Rev. E*, **63**, 016610 (2001);
M. Peccianti, C. Conti, and G. Assanto, *Phys. Rev. E*, **68**, 025602 (2003);
W. Krolikowski *et al.*, *J. Opt. B: Quantum Semiclass. Opt.*, **6**, S288 (2004).
20. D. Mihalache, *Rom. Rep. Phys.*, **59**, 515 (2007).
21. Y. V. Kartashov, L. Torner, V. A. Vysloukh, D. Mihalache, *Opt. Lett.*, **31**, 1483 (2006).
22. D. Mihalache *et al.*, *Phys. Rev. E*, **74**, 066614 (2006).
23. D. Briedis *et al.*, *Opt. Express*, **13**, 435 (2005);
A. I. Yakimenko, Y. A. Zaliznyak, Y. Kivshar, *Phys. Rev. E*, **71**, 065603 (2005);
A. I. Yakimenko, V. M. Lashkin, O. O. Prikhodko, *Phys. Rev. E*, **73**, 066605 (2006);
V. M. Lashkin, *Phys. Rev. A*, **75**, 043607 (2007).
24. D. Mihalache *et al.*, *Phys. Rev. E*, **73**, 025601 (2006);
Yu. A. Zaliznyak, A. I. Yakimenko, *Phys. Lett. A*, **372**, 2862 (2008).
25. D. Rozas, Z. S. Sacks, G. A. Swartzlander, *Phys. Rev. Lett.*, **79**, 3399 (1997).
26. D. Mihalache *et al.*, *Phys. Rev. E*, **67**, 056608 (2003);
D. Mihalache *et al.*, *J. Opt. B: Quantum Semiclassical Opt.*, **6**, S341 (2004);
M. J. Paz-Alonso, H. Michinel, *Phys. Rev. Lett.*, **94**, 093901 (2005).
27. L.-C. Crasovan *et al.*, *Phys. Rev. E*, **66**, 036612 (2002);
L.-C. Crasovan *et al.*, *Phys. Rev. A*, **68**, 063609 (2003);
T. Mizushima, N. Kobayashi, K. Machida, *Phys. Rev. A*, **70**, 043613 (2004);
M. Mottonen, S. M. M. Virtanen, T. Isoshima, M. M. Salomaa, *Phys. Rev. A*, **71**, 033626 (2005).
28. M. Soljacic, S. Sears, M. Segev, *Phys. Rev. Lett.*, **81**, 4851 (1998);
A. S. Desyatnikov, Y. S. Kivshar, *Phys. Rev. Lett.*, **87**, 033901 (2001).
29. Y. J. He, H. H. Fan, J. W. Dong, H. Z. Wang, *Phys. Rev. E*, **74**, 016611 (2006);
Y. J. He, B. A. Malomed, H. Z. Wang, *Opt. Express*, **15**, 17502 (2007);
Y. J. He, B. A. Malomed, D. Mihalache, H. Z. Wang, *Phys. Rev. A*, **77**, 043826 (2008).
30. A. S. Desyatnikov, Y. S. Kivshar, *Phys. Rev. Lett.*, **88**, 053901 (2002);
Y. V. Kartashov *et al.*, *Phys. Rev. Lett.*, **89**, 273902 (2002);
L.-C. Crasovan *et al.*, *Phys. Rev. E*, **67**, 046610 (2003);
D. Mihalache *et al.*, *Phys. Rev. E*, **68**, 046612 (2003);
D. Mihalache *et al.*, *J. Opt. B: Quantum Semiclassical Opt.*, **6**, S333 (2004).

31. A. S. Desyatnikov, A. A. Sukhorukov, Yu. S. Kivshar, *Phys. Rev. Lett.*, **95**, 203904 (2005);
V. M. Lashkin, A. I. Yakimenko, O. O. Prikhodko, *Phys. Lett. A*, **366**, 422 (2007);
V. M. Lashkin, *Phys. Rev. A*, **77**, 025602 (2008);
V. M. Lashkin, *Phys. Rev. A*, **78**, 033603 (2008).
32. X. Liu, L. J. Qian, F. W. Wise, *Phys. Rev. Lett.*, **82**, 4631 (1999).
33. D. Mihalache *et al.*, *Phys. Rev. E*, **70**, 055603 (2004); *Phys. Rev. Lett.*, **95**, 023902 (2005); *Phys. Rev. A*, **72**, 021601 (2005); *Phys. Rev. E*, **74**, 047601 (2006).
34. H. Leblond, B. A. Malomed, D. Mihalache *Phys. Rev. E*, **76**, 026604 (2007).
35. I. S. Aranson, L. Kramer, *Rev. Mod. Phys.*, **74**, 99 (2002);
P. Mandel, M. Tlidi, *J. Opt. B: Quantum Semiclass. Opt.*, **6**, R60 (2004);
B. A. Malomed, in *Encyclopedia of Nonlinear Science*, p. 157, A. Scott (Ed.), Routledge, New York, 2005.
36. L.-C. Crasovan, B. A. Malomed, D. Mihalache, *Phys. Rev. E*, **63**, 016605 (2001);
L.-C. Crasovan, B. A. Malomed, D. Mihalache, *Phys. Lett. A*, **289**, 59 (2001).
37. D. Mihalache *et al.*, *Phys. Rev. Lett.*, **97**, 073904 (2006).
38. D. Mihalache, D. Mazilu, F. Lederer, H. Leblond, B. A. Malomed, *Phys. Rev. A*, **75**, 033811 (2007);
D. Mihalache *et al.*, *Phys. Rev. A*, **76**, 045803 (2007).
39. D. Mihalache, D. Mazilu, F. Lederer, Y. S. Kivshar, *Phys. Rev. A*, **77**, 043828 (2008).
40. D. Mihalache, D. Mazilu, F. Lederer, Y. S. Kivshar, *Phys. Rev. E*, **78**, 056602 (2008).
41. P. Grelu, J. M. Soto-Crespo, N. Akhmediev, *Opt. Express*, **13**, 9352 (2005);
J. M. Soto-Crespo, N. Akhmediev, P. Grelu, *Phys. Rev. E*, **74**, 046612 (2006);
J. M. Soto-Crespo, P. Grelu, N. Akhmediev, *Opt. Express*, **14**, 4013 (2006);
N. Akhmediev, J. M. Soto-Crespo, P. Grelu, *Chaos*, **17**, 037112 (2007).
42. V. Skarka, N. B. Aleksić, *Phys. Rev. Lett.*, **96**, 013903 (2006).
43. D. Mihalache, *Cent. Eur. J. Phys.*, **6**, 582 (2008);
D. Mihalache, D. Mazilu, *Rom. Rep. Phys.*, **60**, 749 (2008).
44. D. Mihalache, D. Mazilu, F. Lederer, H. Leblond, B. A. Malomed, *Phys. Rev. A*, **77**, 033817 (2008); *Phys. Rev. E*, **78**, 056601 (2008).
45. W. J. Tomlinson, *Opt. Lett.*, **5**, 323 (1980);
V. M. Agranovich, V. S. Babichenko, V. Y. Chernyak, *JETP Lett.*, **32**, 512 (1980).
46. V. K. Fedyanin, D. Mihalache, *Z. Phys. B*, **47**, 167 (1982);
D. Mihalache, R. G. Nazmitdinov, V. K. Fedyanin, *Physica Scripta*, **29**, 269 (1984);
D. Mihalache, D. Mazilu, H. Totia, *Physica Scripta*, **30**, 335 (1984).
47. U. Langbein, F. Lederer, H.-E. Ponath, *Opt. Commun.*, **46**, 167 (1983).
48. G. I. Stegeman, C. T. Seaton, J. Chilwell, S. D. Smith, *Appl. Phys. Lett.*, **44**, 830 (1984).
49. N. N. Akhmediev, V. I. Korneyev, Y. V. Kuzmenko, *Zh. Eksp. Teor. Fiz.*, **88**, 107 (1985);
Sov. Phys. JETP, **61**, 62 (1985).
50. F. Lederer, D. Mihalache, *Solid State Commun.*, **59**, 151 (1986);
D. Mihalache, D. Mazilu, F. Lederer, *Opt. Commun.*, **59**, 391 (1986);
D. Mihalache *et al.*, *Opt. Lett.*, **12**, 187 (1987).
51. D. Mihalache, M. Bertolotti, C. Sibilìa, *Prog. Opt.*, **27**, 229 (1989).
52. A. D. Boardman, P. Egan, F. Lederer, U. Langbein, D. Mihalache, "Third-order nonlinear electromagnetic TE and TM guided waves", in: *Nonlinear Surface Electromagnetic Phenomena*, H.-E. Ponath, and G. I. Stegeman (eds.), Elsevier Science Publishers B.V., Amsterdam, 1991, pp. 73–287.
53. F. Lederer, L. Leine, R. Muschall, T. Peschel, C. Schmidt-Hattenberger, U. Trutschel, A. D. Boardman, C. Wächter, *Opt. Commun.*, **99**, 95 (1993).

54. K. G. Makris, S. Suntsov, D. N. Christodoulides, G. I. Stegeman, A. Haché, *Opt. Lett.*, **30**, 2466 (2005).
55. Ya. V. Kartashov, V. V. Vysloukh, L. Torner, *Phys. Rev. Lett.*, **96**, 073901 (2006).
56. S. Suntsov, K. G. Makris, D. N. Christodoulides, G. I. Stegeman, A. Haché, R. Morandotti, H. Yang, G. Salamo, M. Sorel, *Phys. Rev. Lett.*, **96**, 063901 (2006).
57. C. R. Rosberg, D. N. Neshev, W. Krolikowski, A. Mitchell, R. A. Vicencio, M. I. Molina, Yu. S. Kivshar, *Phys. Rev. Lett.*, **97**, 083901 (2006).
58. M. I. Molina, R. A. Vicencio, Yu. S. Kivshar, *Opt. Lett.*, **31**, 1693 (2006).
59. Y. V. Kartashov, L. Torner, and V. A. Vysloukh, *Opt. Lett.* **31**, 2595 (2006);
Y. V. Kartashov, F. Ye, V. A. Vysloukh, L. Torner, *Opt. Lett.*, **32**, 2260 (2007);
M. I. Molina, Y. V. Kartashov, L. Torner, Yu. S. Kivshar, *Opt. Lett.*, **32**, 2668 (2007).
60. Y. Kominis, A. Papadopoulos, K. Hizanidis, *Opt. Express*, **15**, 10041 (2007).
61. Z. Xu, Yu. S. Kivshar, *Opt. Lett.*, **33**, 2551 (2008).
62. E. Smirnov, M. Stepić, C. E. Rütter, D. Kip, V. Shandarov, *Opt. Lett.*, **31**, 2338 (2006).
63. B. Alfassi, C. Rotschild, O. Manela, M. Segev, D. N. Christodoulides, *Phys. Rev. Lett.*, **98**, 213901 (2007).
64. A. Szameit, Y. V. Kartashov, F. Dreisow, M. Heinrich, T. Pertsch, S. Nolte, A. Tünnermann, V. A. Vysloukh, L. Torner, *Opt. Lett.*, **33**, 1132 (2008).
65. X. Wang, A. Samodurov, Z. Chen, *Opt. Lett.*, **33**, 1240 (2008).
66. S. Suntsov *et al.*, *J. Nonl. Opt. Phys. & Mat.*, **16**, 401 (2007);
F. Lederer, G. I. Stegeman, D. N. Christodoulides, G. Assanto, M. Segev, Y. Silberberg, *Phys. Rep.*, **463**, 1 (2008);
Yu. S. Kivshar, *Laser Phys. Lett.*, **5**, 703 (2008).
67. D. Mihalache *et al.*, *Opt. Express*, **15**, 589 (2007); *Opt. Lett.*, **32**, 2091 (2007); *Opt. Express*, **15**, 10718 (2007); *Opt. Lett.*, **32**, 3173 (2007).
68. A. B. Aceves, C. De Angelis, A. M. Rubenchik, S. K. Turitsyn, *Opt. Lett.*, **19**, 329 (1994);
E. W. Laedke, K.H. Spatschek, S. K. Turitsyn, *Phys. Rev. Lett.*, **73**, 1055 (1994);
A. B. Aceves, G. G. Luther, C. De Angelis, A. M. Rubenchik, S. K. Turitsyn, *Phys. Rev. Lett.*, **75**, 73 (1995);
A. V. Buryak, N. N. Akhmediev, *IEEE J. Quantum Electron.*, **31**, 682 (1995).
69. Z. Xu, Y. V. Kartashov, L. C. Crasovan, D. Mihalache, L. Torner, *Phys. Rev. E*, **70**, 066618 (2004).
70. N. K. Efremidis, D. N. Christodoulides, *Phys. Rev. E*, **67**, 026606 (2003).
71. E. A. Ultanir, G. I. Stegeman, D. Michaelis, C. H. Lange, F. Lederer, *Phys. Rev. Lett.*, **90**, 253903 (2003).
72. U. Peschel, O. Egorov, F. Lederer, *Opt. Lett.*, **29**, 1909 (2004).
73. N. K. Efremidis, D. N. Christodoulides, K. Hizanidis, *Phys. Rev. A*, **76**, 043839 (2007).
74. Yu. V. Bludov, V. V. Konotop, *Phys. Rev. E*, **76**, 046604 (2007).
75. Q. E. Hoq, R. Carretero-Gonzalez, P. G. Kevrekidis, B. A. Malomed, D. J. Frantzeskakis, Yu. V. Bludov, V. V. Konotop, *Phys. Rev. E*, **78**, 036605 (2008).
76. C. J. Benton, A. V. Gorbach, D. V. Skryabin, *Phys. Rev. A*, **78**, 033818 (2008).
77. H. Leblond, B. A. Malomed, D. Mihalache, *Phys. Rev. A*, **77**, 063804 (2008).
78. N. C. Panoiu, R. M. Osgood, B. A. Malomed, *Opt. Lett.*, **31**, 1097 (2006);
N. C. Panoiu, B. A. Malomed, R. M. Osgood, *Phys. Rev. A*, **78**, 013801 (2008).
79. F. Kh. Abdullaev, Yu. V. Bludov, S. V. Dmitriev, P. G. Kevrekidis, V. V. Konotop, *Phys. Rev. E*, **77**, 016604 (2008).
80. K. G. Makris, J. Hudock, D. N. Christodoulides, G. I. Stegeman, O. Manela, M. Segev, *Opt. Lett.*, **31**, 2774 (2006).

-
81. M. I. Molina, Yu. S. Kivshar, *Phys. Lett. A*, **362**, 280 (2007);
A. A. Sukhorukov, Yu. S. Kivshar, *Opt. Lett.* **27**, 2112 (2002);
R. A. Vicencio, S. Flach, M. I. Molina, Yu. S. Kivshar, *Phys. Lett. A*, **364**, 274 (2007).
82. R. Morandotti, D. Mandelik, Y. Silberberg, J. S. Aitchison, M. Sorel, D. N. Christodoulides, A. A. Sukhorukov, Yu. S. Kivshar, *Opt. Lett.* **29**, 2890 (2004).
83. K. G. Makris, J. Hudock, D. N. Christodoulides, G. Stegeman, O. Manela, M. Segev, *Opt. Lett.*, **31**, 2774 (2006).
84. H. Susanto, P. G. Kevrekidis, B. A. Malomed, R. Carretero-González, D. J. Franzeskakis, *Phys. Rev. E*, **75**, 056605 (2007).
85. X. Wang, A. Bezryadina, Z. Chen, K. G. Makris, D. N. Christodoulides, G. I. Stegeman, *Phys. Rev. Lett.*, **98**, 123903 (2007).
86. A. Szameit, Y. V. Kartashov, F. Dreisow, T. Pertsch, S. Nolte, A. Tünnermann, L. Torner, *Phys. Rev. Lett.*, **98**, 173903 (2007);
A. Szameit, Y. V. Kartashov, F. Dreisow, M. Heinrich, T. Pertsch, S. Nolte, A. Tünnermann, V. A. Vysloukh, F. Lederer, L. Torner, *Phys. Rev. Lett.*, **102**, 063902 (2009).
87. D. Mihalache, D. Mazilu, F. Lederer, Y. S. Kivshar, *Phys. Rev. A*, **79**, 013811 (2009).